Supplementary Information

Label Free Absolute Quantitation of Oligosaccharides using Multiple Reaction Monitoring

Qiuting Hong,[a] L. Renee Ruhaak,[a] Sarah M. Totten,[a] Jennifer T. Smilowitz,[b,c] J. Bruce German,[b,c] Carlito B. Lebrilla[a,b,*]

[a]Department of Chemistry, University of California, Davis, California, 95616, United States

[b]Foods for Health Institute, University of California, Davis, California, 95616, United States

[c]Department of Food Science and Technology, University of California, Davis, California, 95616, United States

*To whom correspondence should be addressed

Carlito B. Lebrilla
One Shields Avenue
Davis, CA 95616, USA
Tel.: +1-530-752-5504
Fax: +1-530-752-8995
E-mail: cblebrilla@ucdavis.edu

Table of Content

EXPERIMENTAL PROCEDURES

Samples and Materials. Lacto-N-tetraose (LNT), lacto-N-fucopentaose I (LNFP-I), sialyllacto-N-tetraose c (LSTc), 3'-sialyllactose (3'-SL) and 6'-sialyllactose (6'-SL) standards were purchased from Carbosynth Limited (Berkshire, UK). 2'-fucosyllactose (2'-FL) and lacto-N-hexaose (LNH) standards were purchased from Sigma-Aldrich (St. Louis, MO, USA). Sodium borohydride ($NaBH_4$, 98%) and formic acid were purchased from Sigma-Aldrich (St. Louis, MO, USA). Graphitized carbon cartridges (GCC, 150 mg bed weight, 4 mL cartridge volume) were purchased from Grace (Deerfield, IL, USA). Milk samples were obtained from twenty healthy women who gave birth to healthy full term infants enrolled in the UC Davis Foods for Health Institute Lactation Study. Participants were instructed to write on all sample tubes the time, and date of collection. Milk samples were collected in the morning on day 35 postpartum (except for milk from mother ID #1038, which was collected on day 28) using a modified published method[1] involving milk collection from one breast using a Harmony manual breast pump (Medela Inc., McHenry, IL) by the participant 2−4 h after feeding her infant. Participants fully pumped one breast into a bottle, inverted 6 times, transferred 12 mL into a 15 mL polypropylene tube, and subsequently froze the sample in the kitchen freezer (−20 °C). Samples were picked up from the participants' homes on a biweekly basis, transported to the lab on dry ice, and stored at −80 °C until processing. The participants' secretor status was determined by measuring specific fucosylated HMO structures in their milk as previously described.[2] Ten secretor and ten nonsecretor participants were chosen for this study. The UC Davis Institutional Review Board approved all aspects of the study and informed consent was obtained from all subjects. This trial was registered on clinicaltrials.gov (ClinicalTrials.gov Identifier: NCT01817127).

Standard Calibration and Standard Addition Curves. A serial dilution was performed for the HMO standards to create the standard calibration curve for absolute quantitation. The concentrations studied

are from 0.833 μg/mL to $1.67x10^2$ μg/mL for 2'-FL, LNT, LNFP-I, from 0.833 μg/mL to 83.3 μg/mL for 3'-SL, 6'-SL and LSTc, and from 0.500 μg/mL to $1.00x10^2$ μg/mL for LNH.

A standard addition experiment was performed for one of the milk samples (mother ID# 1035). Briefly, varying amount of HMO standards were added into the 20x diluted extracted milk oligosaccharide sample to create a standard addition calibration curve. Three concentration levels were performed besides the non-spiked sample. They are 20.8, 31.3 and 41.7 μg/mL for 2'-FL, 5.00, 10.4 and 15.6 μg/mL for LNT, 4.17, 6.25 and 8.33 μg/mL for LNFP-I, 0.500, 1.00 and 2.00 μg/mL for LNH, 2.08, 4.17 and 6.25 μg/mL for 6'-SL, 3.13, 5.00, and 6.25 μg/mL for 3'-SL, 1.04, 1.56 and 2.08 μg/mL for LSTc. These specific concentrations were chosen so that their MRM responses were within 3 times of the non-spiked sample.

LC Gradients. The LC separations were performed using a binary gradient at 0.2 mL/min flow rate: solvent A of 3% acetonitrile, 0.1% formic acid; solvent B of 90% acetonitrile, 0.1% formic acid in nano pure water (v/v). The 55-min gradient was programmed as follows: 0−20 min, 0−16% B; 20−30 min, 16−44% B; 30−35 min, 44−100% B; 35−40 min, 100% B; 40−41 min, 100−0%; 41−45 min, 0% B. The 10-min gradient used in instrument optimization was programmed as follows: 0−2 min, 5−40% B; 2−3 min, 40−100% B; 3−5 min, 100% B; 5−7 min, 100-5% B; 7−10 min, 5% B.

Data Analysis. MRM signal (peak area) was extracted and a linear regression was performed to examine the correlation between the MRM response (*y*, ion counts) and the HMO concentration (*x*, μg/mL) using Agilent MassHunter Quantitative B.05.02. The closeness of the fit was evaluated by the coefficient of determination, R^2. HMO identifications were performed based on the retention time and ion abundances.

Table S-1. Dynamic MRM transition list

Composition [a] (Hex:HexNAc:Fuc:Neu5Ac)	mass (Da)	Precursor Ion (*m/z*)	Product Ion [b] (*m/z*)	Isomers	Retention time [c] (min)	Collision Energy (eV)
2010	490.19	491.2	345.2, 183.1	2'-FL	13.8±1.4	6
				3'-FL	2.0±3.0	6
3000	506.18	507.3	345.2, 183.1	3000 a	11.7±1.4	10
				3000 b	12.1±1.4	10
				3000 c	15.8±1.4	10
2001	635.23	636.3	292.1, 454.3	6'-SL	17.5±4.0	12
				3'-SL	26.9±4.0	12
2020	636.25	637.3	491.2, 183.1	LDFT	15.9±1.5	6
1101	676.25	677.3	386.2, 224.1	6'-SLN	17.5±4.0	10
				3'-SLN	27.5±4.0	10
3100	709.26	710.3	366.2, 204.1	LNT, LNnT	15.6±1.8	15
3110	855.32	856.3	512.2, 366.2	LNFP-I	14.9±1.5	10
				LNFP-II	11.7±1.5	10
				LNFP-V	16.0±1.5	10
3101	1000.36	1001.4	657.1, 292.1	LST a, b, c	26.5±7.0	15
3120	1001.38	501.7	512.2, 204.1	LNDFH I, II	11.5±2.2	10
4200	1074.40	538.4	366.2, 204.1	LNH, LNnH	18.8±2.2	12
3111	1146.42	574.2	366.2, 292.1	3111	24.0±6.0	15
3220	1204.46	603.2	512.2, 366.2	3220	11.7±1.5	15
4210	1220.45	611.2	512.2, 366.2	MFLNH, IFLNH	18.0±3.0	15
4300	1277.4	639.8	204.1, 366.2	4300	17.7±2.0	20
4201	1365.49	683.8	366.2, 292.1	4201	27.0±7.0	15
4220	1366.51	684.3	512.2, 366.2	DFLNH b	14.4±1.5	20
				DFLNH a	16.0±1.5	20
				DFLNH c	20.3±1.5	20
4211	1511.55	756.8	366.2, 292.1	4211	25.8±8.5	15
4230	1512.57	757.3	512.2, 366.2	TFLNH	14.4±1.5	10
				4230	19.8±1.5	10
5310	1585.59	793.8	512.2, 366.2	5310	20.0±6.0	22
4221	1657.61	829.8	366.2, 292.1	4221	26.0±8.0	15
5301	1730.62	866.3	366.2, 292.1	5301	27.0±6.0	25
5320	1731.64	866.8	512.2, 366.2	5320	19.5±6.0	25
5311	1876.68	939.3	366.2, 292.1	5311	26.5±7.0	25
5330	1877.70	939.9	512.2, 366.2	5330	16.0±5.0	25
6410	1950.72	976.4	512.2, 366.2	6410	22.8±4.0	30
5321	2022.74	1012.4	366.2, 292.1	5321	25.5±7.5	15
5340	2023.76	1012.9	512.2, 366.2	5340	18.1±2.0	25
6401	2095.76	1048.9	366.2, 292.1	6401	27.2±5.0	25
6420	2096.78	1049.4	512.2, 366.2	6420	22.5±5.0	25
5331	2168.80	1085.4	366.2, 292.1	5331	25.0±8.0	25
6430	2242.83	748.6	512.2, 366.2	6430	21.0±4.0	20
6440	2388.89	1195.5	512.2, 366.2	6440	19.3±1.5	25

a. Monosaccharide composition 5Hex:3HexNAc:2Fuc:1Neu5Ac represented as 5321. Hex: hexose, HexNAc: N-acetylhexosamine; Fuc: fucose, Neu5Ac: N-acetylneuraminic acid.

b. Product ions were monitored for the same compound.

c. Compounds with isomers were monitored either in several different time windows or in one extended time window.

Figure S-1

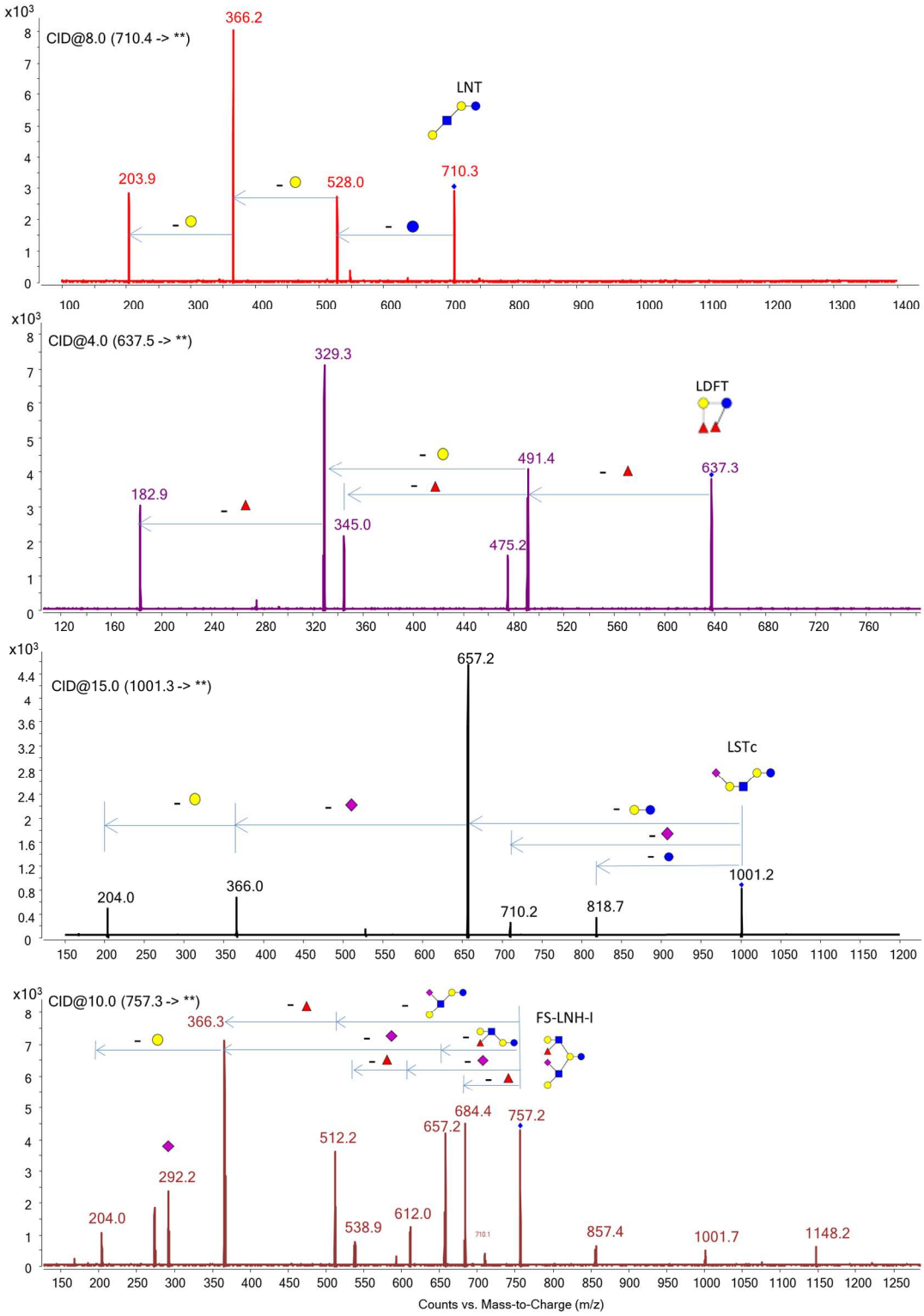

Figure S-1: HMO fragmentation patterns using collision-induced dissociation in a quadrupole show some common carbohydrate fragment ions such as *m/z* 366.2 (GlcNAc−Gal), 204.1 (GlcNAc), 183.1 (Glc,

reducing end), 512.2 (Fuc–GlcNAc–Gal), 292.1 (Neu5Ac), and 657.1 (Neu5Ac–GlcNAc–Gal). (●) Glc (●) Gal (■) GlcNAc (■) GalNAc (▲) Fuc (♦) Neu5Ac

Figure S-2

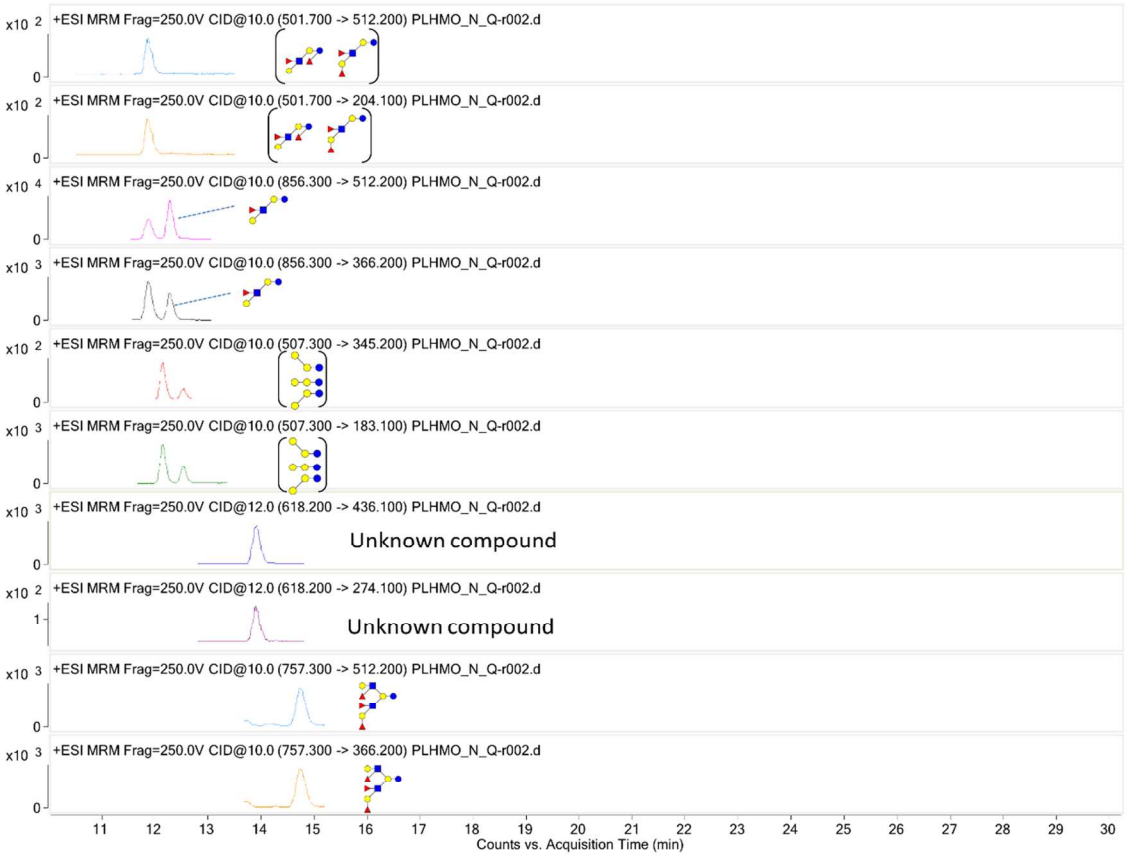

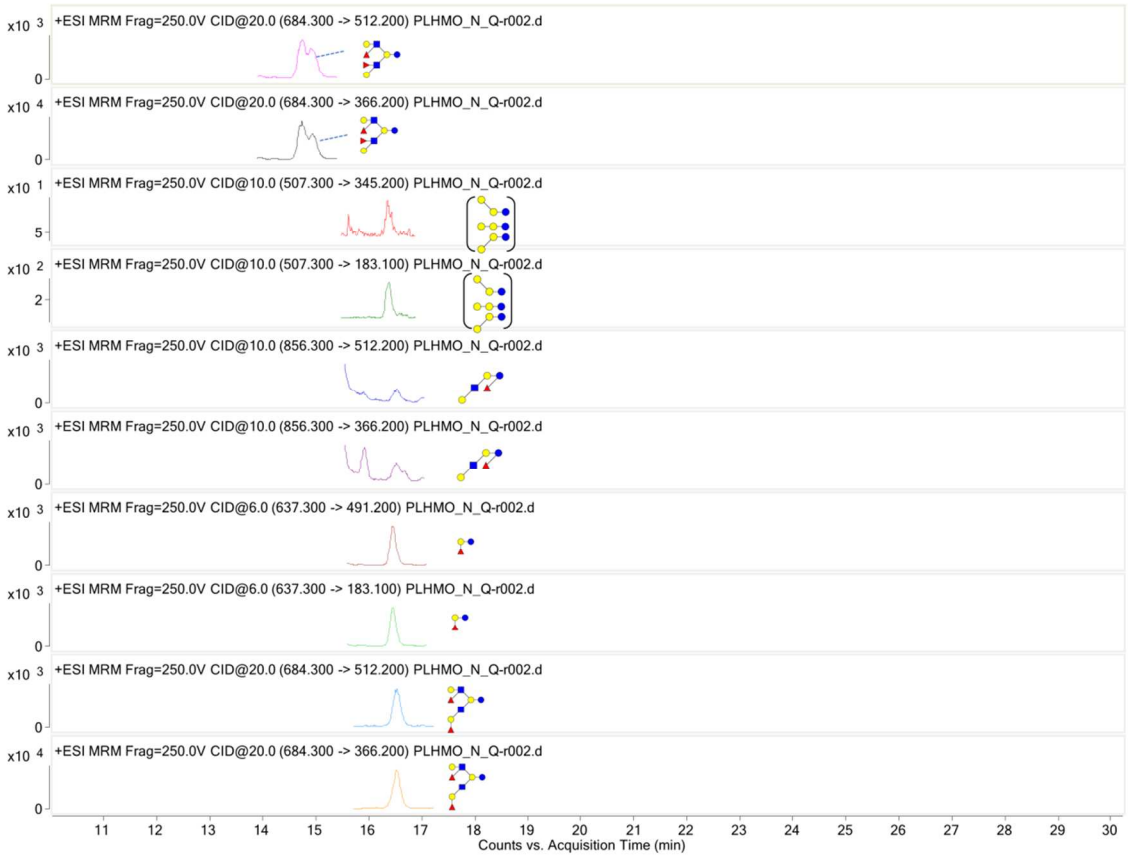
x10 3 +ESI MRM Frag=250.0V CID@20.0 (684.300 -> 512.200) PLHMO_N_Q-r002.d
x10 4 +ESI MRM Frag=250.0V CID@20.0 (684.300 -> 366.200) PLHMO_N_Q-r002.d
x10 1 +ESI MRM Frag=250.0V CID@10.0 (507.300 -> 345.200) PLHMO_N_Q-r002.d
x10 2 +ESI MRM Frag=250.0V CID@10.0 (507.300 -> 183.100) PLHMO_N_Q-r002.d
x10 3 +ESI MRM Frag=250.0V CID@10.0 (856.300 -> 512.200) PLHMO_N_Q-r002.d
x10 3 +ESI MRM Frag=250.0V CID@10.0 (856.300 -> 366.200) PLHMO_N_Q-r002.d
x10 3 +ESI MRM Frag=250.0V CID@6.0 (637.300 -> 491.200) PLHMO_N_Q-r002.d
x10 3 +ESI MRM Frag=250.0V CID@6.0 (637.300 -> 183.100) PLHMO_N_Q-r002.d
x10 3 +ESI MRM Frag=250.0V CID@20.0 (684.300 -> 512.200) PLHMO_N_Q-r002.d
x10 4 +ESI MRM Frag=250.0V CID@20.0 (684.300 -> 366.200) PLHMO_N_Q-r002.d
11 12 13 14 15 16 17 18 19 20 21 22 23 24 25 26 27 28 29 30
Counts vs. Acquisition Time (min)

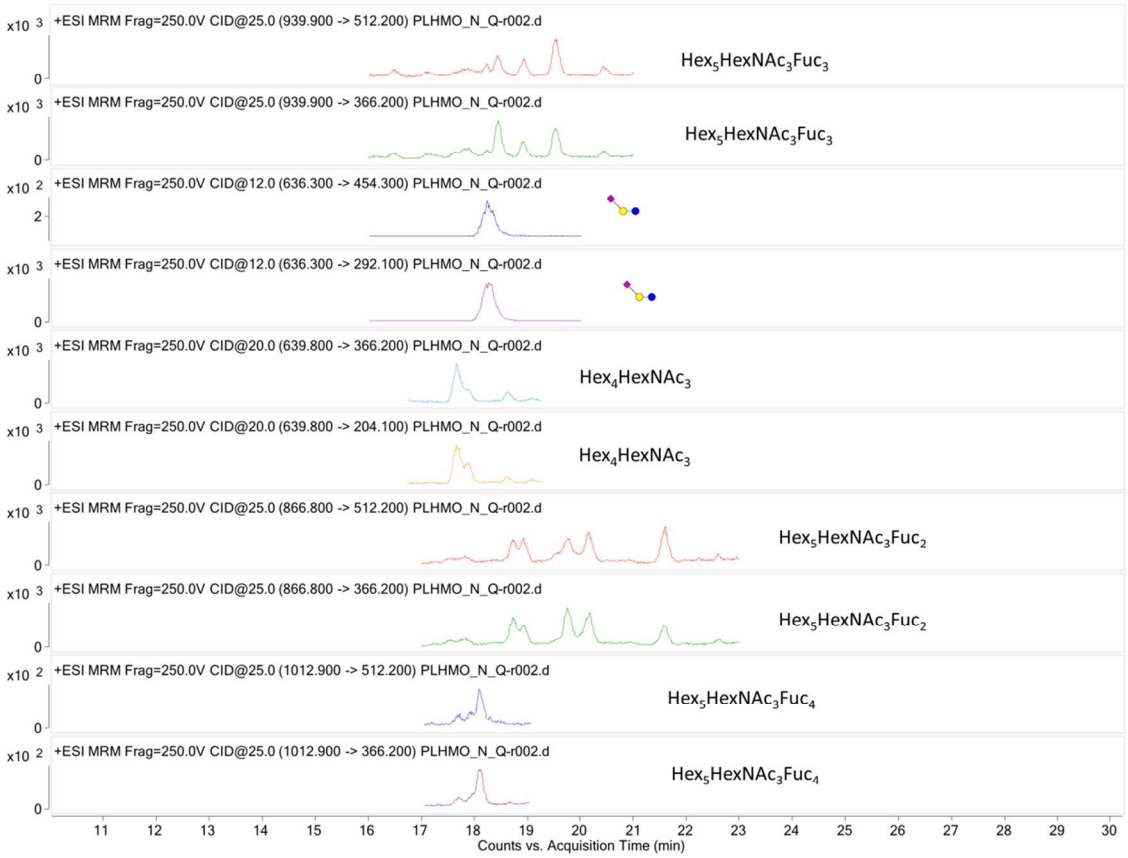
+ESI MRM Frag=250.0V CID@25.0 (939.900 -> 512.200) PLHMO_N_Q-r002.d
Hex5HexNAc3Fuc3
+ESI MRM Frag=250.0V CID@25.0 (939.900 -> 366.200) PLHMO_N_Q-r002.d
Hex5HexNAc3Fuc3
+ESI MRM Frag=250.0V CID@12.0 (636.300 -> 454.300) PLHMO_N_Q-r002.d
+ESI MRM Frag=250.0V CID@12.0 (636.300 -> 292.100) PLHMO_N_Q-r002.d
+ESI MRM Frag=250.0V CID@20.0 (639.800 -> 366.200) PLHMO_N_Q-r002.d
Hex4HexNAc3
+ESI MRM Frag=250.0V CID@20.0 (639.800 -> 204.100) PLHMO_N_Q-r002.d
Hex4HexNAc3
+ESI MRM Frag=250.0V CID@25.0 (866.800 -> 512.200) PLHMO_N_Q-r002.d
Hex5HexNAc3Fuc2
+ESI MRM Frag=250.0V CID@25.0 (866.800 -> 366.200) PLHMO_N_Q-r002.d
Hex5HexNAc3Fuc2
+ESI MRM Frag=250.0V CID@25.0 (1012.900 -> 512.200) PLHMO_N_Q-r002.d
Hex5HexNAc3Fuc4
+ESI MRM Frag=250.0V CID@25.0 (1012.900 -> 366.200) PLHMO_N_Q-r002.d
Hex5HexNAc3Fuc4
11 12 13 14 15 16 17 18 19 20 21 22 23 24 25 26 27 28 29 30
Counts vs. Acquisition Time (min)

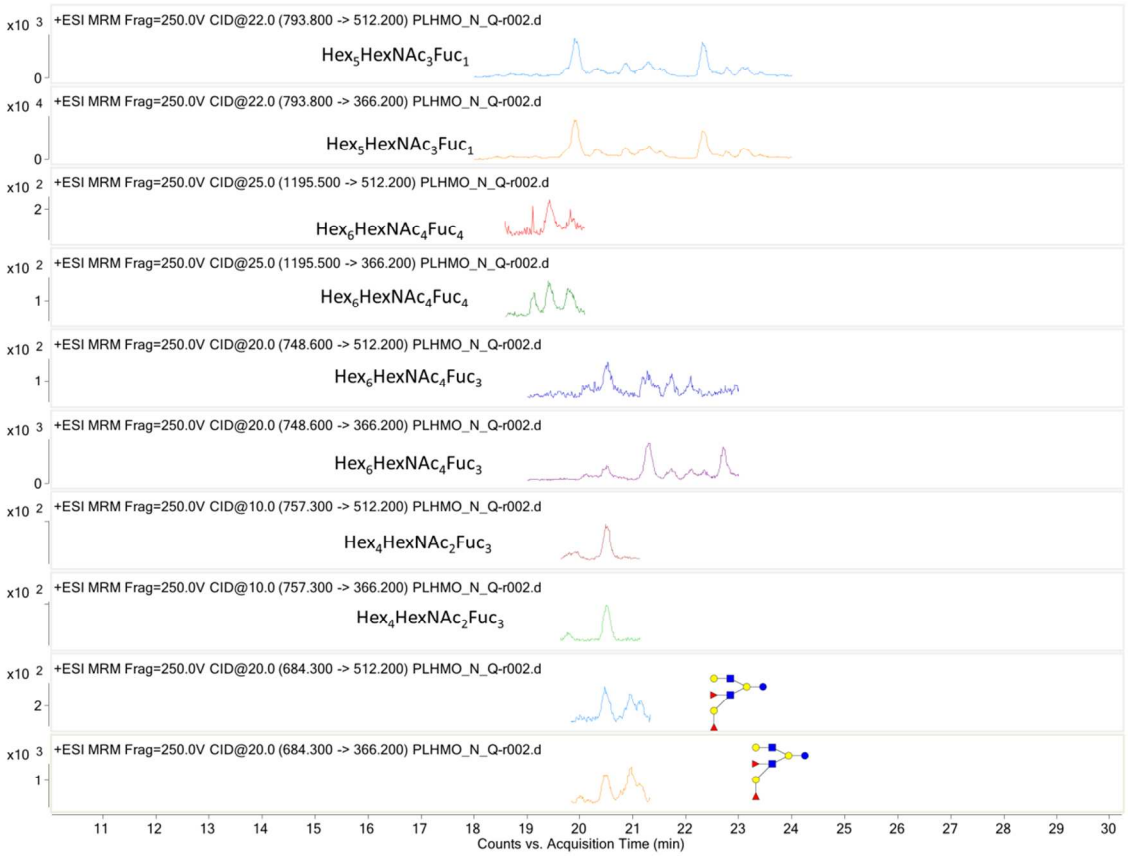
+ESI MRM Frag=250.0V CID@22.0 (793.800 -> 512.200) PLHMO_N_Q-r002.d
Hex5HexNAc3Fuc1
+ESI MRM Frag=250.0V CID@22.0 (793.800 -> 366.200) PLHMO_N_Q-r002.d
Hex5HexNAc3Fuc1
+ESI MRM Frag=250.0V CID@25.0 (1195.500 -> 512.200) PLHMO_N_Q-r002.d
Hex6HexNAc4Fuc4
+ESI MRM Frag=250.0V CID@25.0 (1195.500 -> 366.200) PLHMO_N_Q-r002.d
Hex6HexNAc4Fuc4
+ESI MRM Frag=250.0V CID@20.0 (748.600 -> 512.200) PLHMO_N_Q-r002.d
Hex6HexNAc4Fuc3
+ESI MRM Frag=250.0V CID@20.0 (748.600 -> 366.200) PLHMO_N_Q-r002.d
Hex6HexNAc4Fuc3
+ESI MRM Frag=250.0V CID@10.0 (757.300 -> 512.200) PLHMO_N_Q-r002.d
Hex4HexNAc2Fuc3
+ESI MRM Frag=250.0V CID@10.0 (757.300 -> 366.200) PLHMO_N_Q-r002.d
Hex4HexNAc2Fuc3
+ESI MRM Frag=250.0V CID@20.0 (684.300 -> 512.200) PLHMO_N_Q-r002.d
+ESI MRM Frag=250.0V CID@20.0 (684.300 -> 366.200) PLHMO_N_Q-r002.d
11 12 13 14 15 16 17 18 19 20 21 22 23 24 25 26 27 28 29 30
Counts vs. Acquisition Time (min)

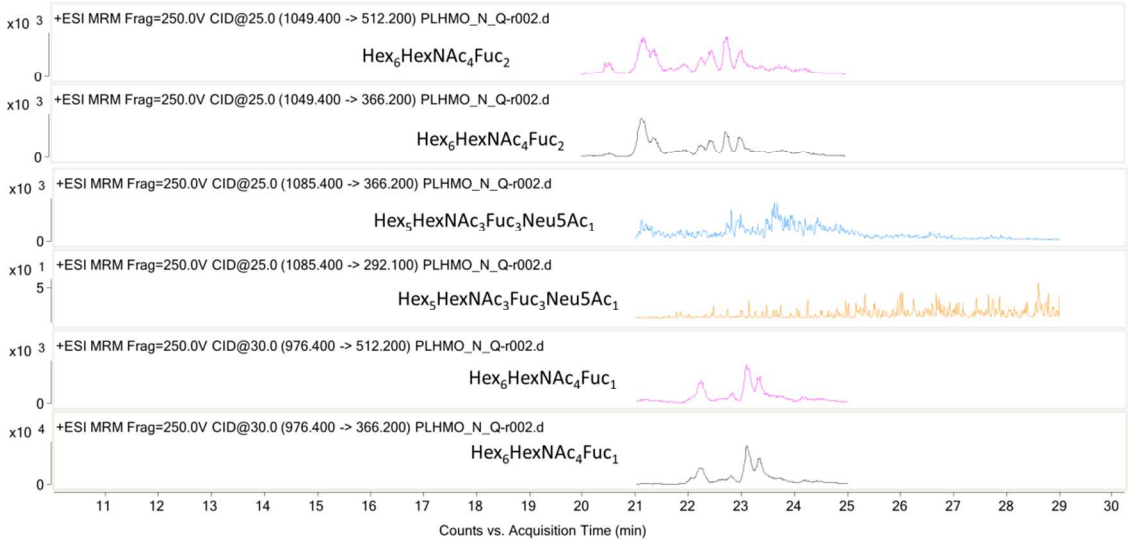
+ESI MRM Frag=250.0V CID@25.0 (1049.400 -> 512.200) PLHMO_N_Q-r002.d
Hex6HexNAc4Fuc2
+ESI MRM Frag=250.0V CID@25.0 (1049.400 -> 366.200) PLHMO_N_Q-r002.d
Hex6HexNAc4Fuc2
+ESI MRM Frag=250.0V CID@25.0 (1085.400 -> 366.200) PLHMO_N_Q-r002.d
Hex5HexNAc3Fuc3Neu5Ac1
+ESI MRM Frag=250.0V CID@25.0 (1085.400 -> 292.100) PLHMO_N_Q-r002.d
Hex5HexNAc3Fuc3Neu5Ac1
+ESI MRM Frag=250.0V CID@30.0 (976.400 -> 512.200) PLHMO_N_Q-r002.d
Hex6HexNAc4Fuc1
+ESI MRM Frag=250.0V CID@30.0 (976.400 -> 366.200) PLHMO_N_Q-r002.d
Hex6HexNAc4Fuc1
11 12 13 14 15 16 17 18 19 20 21 22 23 24 25 26 27 28 29 30
Counts vs. Acquisition Time (min)

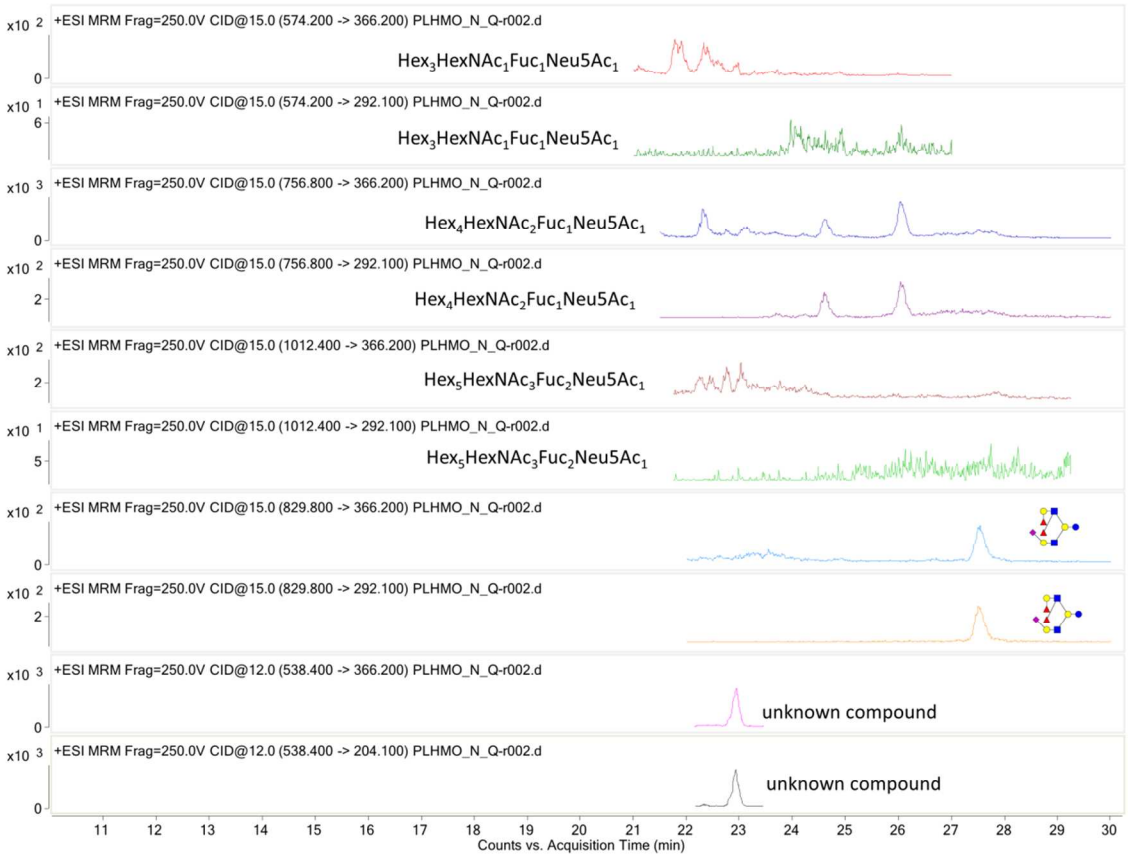
+ESI MRM Frag=250.0V CID@15.0 (574.200 -> 366.200) PLHMO_N_Q-r002.d
Hex3HexNAc1Fuc1Neu5Ac1
+ESI MRM Frag=250.0V CID@15.0 (574.200 -> 292.100) PLHMO_N_Q-r002.d
Hex3HexNAc1Fuc1Neu5Ac1
+ESI MRM Frag=250.0V CID@15.0 (756.800 -> 366.200) PLHMO_N_Q-r002.d
Hex4HexNAc2Fuc1Neu5Ac1
+ESI MRM Frag=250.0V CID@15.0 (756.800 -> 292.100) PLHMO_N_Q-r002.d
Hex4HexNAc2Fuc1Neu5Ac1
+ESI MRM Frag=250.0V CID@15.0 (1012.400 -> 366.200) PLHMO_N_Q-r002.d
Hex5HexNAc3Fuc2Neu5Ac1
+ESI MRM Frag=250.0V CID@15.0 (1012.400 -> 292.100) PLHMO_N_Q-r002.d
Hex5HexNAc3Fuc2Neu5Ac1
+ESI MRM Frag=250.0V CID@15.0 (829.800 -> 366.200) PLHMO_N_Q-r002.d
+ESI MRM Frag=250.0V CID@15.0 (829.800 -> 292.100) PLHMO_N_Q-r002.d
+ESI MRM Frag=250.0V CID@12.0 (538.400 -> 366.200) PLHMO_N_Q-r002.d
unknown compound
+ESI MRM Frag=250.0V CID@12.0 (538.400 -> 204.100) PLHMO_N_Q-r002.d
unknown compound
Counts vs. Acquisition Time (min)

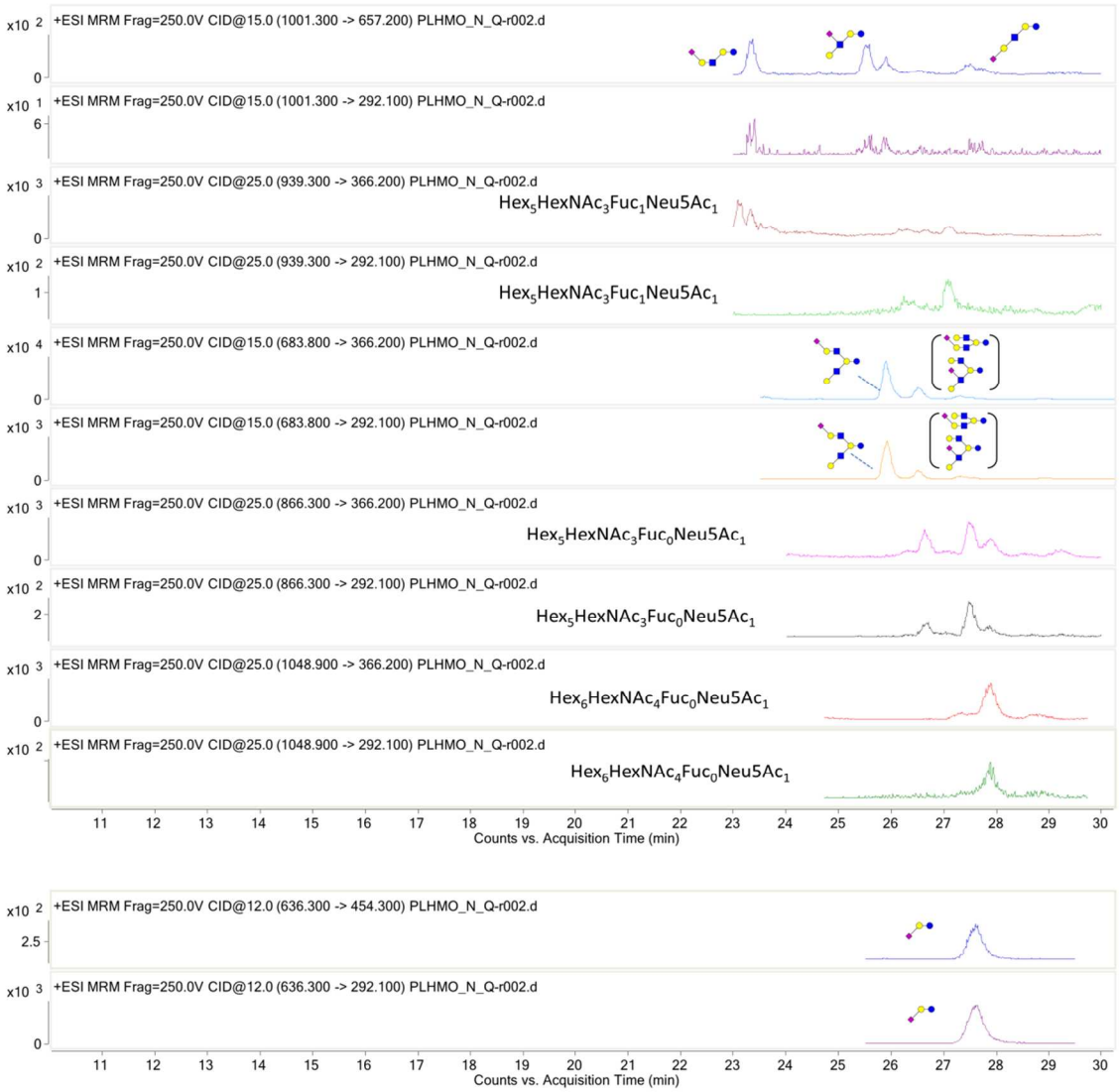

Figure S-2: Individual extract ion chromatograms for **Figure 3b**. (●) Glc (●) Gal (■) GlcNAc (■) GalNAc (▲) Fuc (♦) Neu5Ac

Figure S-3

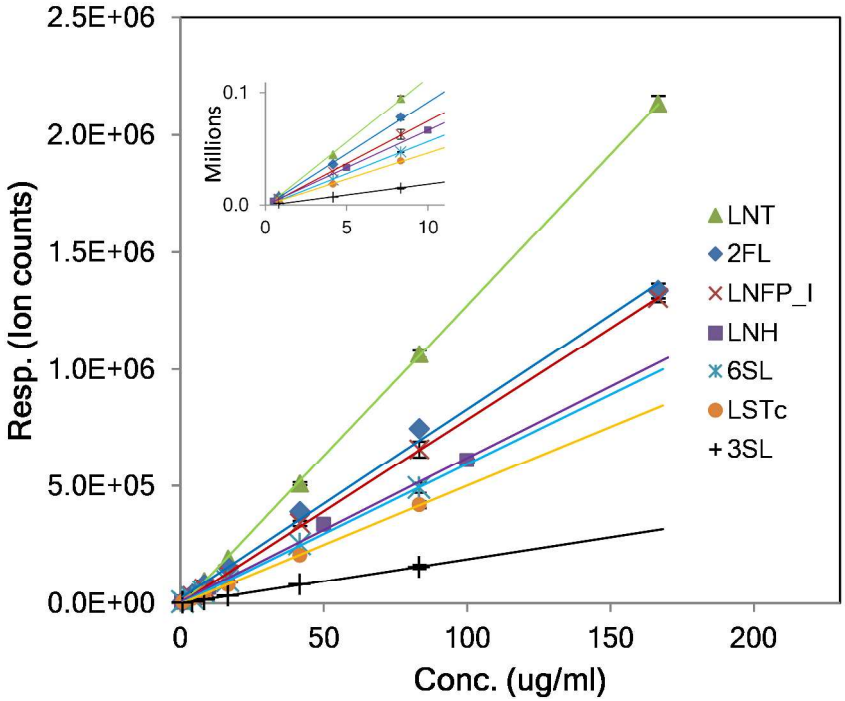

Figure S-3: The concentration studied here was from 8.33×10^{-1} µg/mL to 1.67×10^{2} µg/mL for 2'-FL, LNFP-I, and LNT, from 0.500 µg/mL to 1.00×10^{2} µg/mL for LNH, from 8.33×10^{-1} µg/mL to 8.33×10^{1} µg/mL for LSTc, 3'-SL and 6'-SL. Calibration curves for the seven HMO standards studied show a wide linear range over 2 orders of magnitude. The response of the HMO standards can be fitted to linear equations as follows: (▲) LNT, $y = 12{,}880x - 14{,}067$, $R^2 = 1.000$; (♦) 2'-FL, $y = 8{,}082x + 20{,}297$, $R^2 = 0.996$; (X) LNFP-I, $y = 7{,}851x - 452$, $R^2 = 1.000$; (■) LNH, $y = 6{,}131x + 6{,}239$, $R^2 = 0.998$; (*) 6'-SL, $y = 5{,}950x - 1{,}652$, $R^2 = 1.000$; (●) LSTc, $y = 5{,}041x - 3{,}586$, $R^2 = 1.000$; (+) 3'-SL, $y = 1{,}881x - 184$, $R^2 = 1.000$. The slopes for the 7 HMOs studied are different by a factor of 2 except for 3'-SL. The repeatability of the instrument response was studied by injecting the same sample three times. The result shows a RSD <10% for concentrations at all levels.

Figure S-4

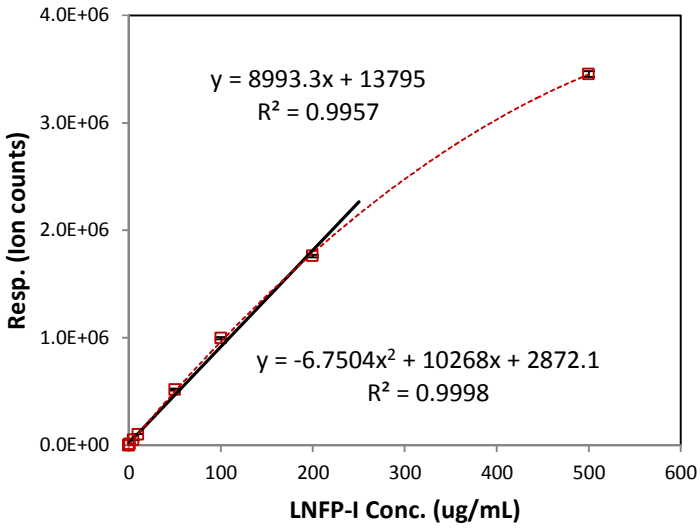

Figure S-4: Calibration curve of LNFP-I in nano pure water. The concentration of LNFP-I studied spanned from 0.001µg/ml to 500 µg/ml. The red dash line was the polynomial fit from 0.001 µg/ml to 500 µg/ml. The fitted equation is $y=6.75x^2 + 10{,}268x + 2{,}872$, $R^2=0.9998$. The black line was the linear fit from 0.001 µg/ml to 200 µg/ml. The linear regression equation is $y= 8993.3x – 13{,}795$, $R^2=0.996$.

Reference

(1) Ferris, A. M.; Jensen, R. G. *J. Pediatr. Gastroenterol. Nutr.* **1984**, *3*, 108-122.
(2) Totten, S. M.; Zivkovic, A. M.; Wu, S.; Ngyuen, U.; Freeman, S. L.; Ruhaak, L. R.; Darboe, M. K.; German, J. B.; Prentice, A. M.; Lebrilla, C. B. *J. Proteome Res.* **2012**, *11*, 6124-6133.